

- [7] A. Cassell, N. Franklin, T. Tomblor, E. Chan, J. Han, H. Dai, *J. Am. Chem. Soc.* **1999**, 121, 7975.
- [8] P. Yang, T. Deng, D. Zhao, P. Feng, D. Pine, B. F. Chmelka, G. M. Whitesides, G. D. Stucky, *Science* **1998**, 282, 2244.
- [9] L. Wang, L. Tao, M. Xie, G. Xu, J. Huang, Y. Xu, *Catal. Lett.* **1993**, 21, 35.
- [10] S. Liu, L. Wang, R. Ohnishi, M. Ichikawa, *J. Catal.* **1999**, 181, 175.
- [11] J. Kong, A. M. Cassell, H. Dai, *Chem. Phys. Lett.* **1998**, 292, 567.
- [12] A. Cassell, J. Raymakers, J. Kong, H. Dai, *J. Phys. Chem.* **1999**, 103, 6484.

## Novel Bioactive Functionally Graded Coatings on Ti6Al4V\*\*

By Jose M. Gomez-Vega, Eduardo Saiz,  
Antoni P. Tomsia,\* Takeo Oku, Katsuki Suganuma,  
Grayson W. Marshall, and Sally J. Marshall

The use of ceramics in medicine has increased tremendously during the past decades, and it is anticipated that the use of bioceramics will increase dramatically during the next millennium. An estimated 11 million people in the United States have at least one medical-device implant.<sup>[1]</sup> Today, more than 500 000 arthroplastic procedures and total joint replacements are performed annually in the U.S. alone.<sup>[2]</sup> Moreover, as the population receiving such implants becomes younger, this number is likely to increase. This has motivated significant effort towards improving implant performance through the design of artificial bone-like materials. A variety of bioceramics have been developed and produced, but (despite their excellent biological performance) only a few of them have been used in clinical applications (mainly in non- or low-load-bearing implants), on account of their poor mechanical strength. As a consequence, metals such as Ti and alloys Co-Cr are being used for implants where high strength is required. At best, they are bioinert. For better osteointegration, metals need to be coated with a bioactive material, and the most common technique is to use plasma-sprayed coatings of hydroxyapatite (HA).<sup>[3,4]</sup> Typically, the plasma-sprayed coatings consist of a mixture of amorphous and crystalline phases.<sup>[5]</sup> The

fast dissolution of the amorphous phase and some of the crystalline products like tricalcium phosphate (TCP) degrade the stability of the coating.<sup>[5]</sup> Further heat treatment to improve crystallinity often results in cracking and loss of adhesion.<sup>[6]</sup> Some of the major causes of failure of HA-coated metal orthopedic and dental implants appear to reside in the coating.<sup>[7]</sup> Clearly, new coatings for implant materials are needed. Indeed, Kasemo and Gold<sup>[8]</sup> suggested that future progress in biomaterials must include the development of coatings with programmed dissolution of multi-layer surfaces. Such surfaces would provide new opportunities to optimize the biomaterial coating surface for different periods of the healing-in phase. This programmed dissolution can then be used to expose different micro-architectures, chemical patterns, and porosities at various times. Fabrication of coatings for medical applications involves a compromise between adhesion, mechanical stability, and bioactivity, but coatings that satisfy all these requirements are extremely difficult to develop.

Graded bioactive glass coatings can provide an answer to that challenge. Graded or layered materials have been used for years in specific applications to improve bonds between dissimilar materials, coating adherence, and compatibility between fibers and matrices in composites.<sup>[9-11]</sup> Recently, such materials have been formally classified as functionally graded materials (FGMs), leading to expanded work on improving their processing and comprehending their properties. By controlling the gradient in the glass composition (i.e., in the glass structure) along the coating, good adhesion to the metal can be combined with rapid biofixation and long-term stability.

As a first step towards the development of graded coatings, a new family of glasses in the SiO<sub>2</sub>-CaO-MgO-Na<sub>2</sub>O-K<sub>2</sub>O-P<sub>2</sub>O<sub>5</sub> system has been developed. The compositions of the glasses are related to that of Bioglass (BG),<sup>[12]</sup> but with MgO and K<sub>2</sub>O substituted for CaO and Na<sub>2</sub>O. These additions alter the thermal expansion and softening points such that enameling can be carried out below the  $\alpha \rightarrow \beta$  transformation of Ti in the alloy Ti6Al4V (955-1010 °C), without generating large thermal stresses. The silica content of the glasses ranges between 45 and 68 wt.-%. The thermal expansion coefficients (CTE) are in the range of  $8.8$  to  $15.1 \times 10^{-6} \text{ °C}^{-1}$ , which includes the CTE of Ti6Al4V ( $\sim 9.6 \times 10^{-6} \text{ °C}^{-1}$ ). The nominal compositions of the glasses and their main thermal properties are listed in Table 1.

The coatings were fabricated using a conventional enameling technique. Because of the high reactivity of Ti alloys, a fast-firing procedure has been developed to control reactivity and provide excellent adhesion (see experimental section). The reaction sequence at the glass/metal interfaces during firing was evaluated using a combination of X-ray diffraction (XRD), scanning electron microscopy (SEM) of cross sections and fracture surfaces, and high-resolution transmission electron microscopy (HRTEM) combined with energy-dispersive spectroscopy (EDS). During

[\*] Dr. A. P. Tomsia, Dr. J. M. Gomez-Vega, Dr. E. Saiz  
Lawrence Berkeley National Laboratory  
Materials Sciences Division  
Berkeley, CA 94720 (USA)  
Dr. T. Oku, Prof. K. Suganuma  
Institute of Scientific and Industrial Research  
Osaka University  
Osaka 567-0047 (Japan)  
Prof. G. W. Marshall, Prof. S. J. Marshall  
University of California  
Department of Restorative Dentistry  
San Francisco, CA 94143-0758 (USA)

[\*\*] This work was supported by the NIH/NIDCR grant 1R01DE11289. Jose M. Gomez-Vega thanks the Spanish Ministry of Education (MEC) for financial support. The Advanced Light Source is supported by the Director, Office of Science, Office of Basic Energy Sciences, Materials Sciences Division, of the U.S. Department of Energy under Contract No. DE-AC03-76SF00098 at Lawrence Berkeley National Laboratory.

Table 1. Glass compositions (in wt.-%) and their thermal properties.

	SiO <sub>2</sub>	Na <sub>2</sub> O	K <sub>2</sub> O	CaO	MgO	P <sub>2</sub> O <sub>5</sub>	CTE [a] [10 <sup>-6</sup> C <sup>-1</sup> ]	T <sub>g</sub> [b] [°C]	T <sub>s</sub> [c] [°C]
Bioglass	45.0	24.5		24.5		6.0	15.1	511	557
6P44-a	44.2	23.6	6.5	12.6	7.1	6.0	15.6	449	503
6P44-b	44.2	17.0	4.6	18.0	10.2	6.0	13.0	516	560
6P44-c	44.2	10.3	2.8	23.4	13.3	6.0	11.3	527	599
6P50	49.8	15.5	4.2	15.6	8.9	6.0	12.2	522	560
6P53-a	52.7	17.0	4.6	12.6	7.1	6.0	12.9	530	565
6P53-b	52.7	10.3	2.8	18.0	10.2	6.0	11.5	531	608
6P55	54.5	12.0	4.0	15.0	8.5	6.0	11.0	548	602
6P57	56.5	11.0	3.0	15.0	8.5	6.0	10.8	557	609
6P61	61.1	10.3	2.8	12.6	7.2	6.0	10.2	564	624
6P68	67.7	8.3	2.2	10.1	5.7	6.0	8.8	565	644

[a] Measured between 200 and 400 °C. [b] Transition temperature. [c] Softening temperature.

heating, gas flows easily through the porous deposited coating, forming a titanium oxide (firing in air) or nitride (firing in N<sub>2</sub>) layer on the alloy surface. When the glass softens and flows, it dissolves the oxides or reacts with the nitrides. Once they have been completely removed, redox reactions at the glass/metal interface occur. A key processing factor is the control of the interfacial reaction between the glass and the alloy. The main reaction is the formation of titanium silicide (3 SiO<sub>2</sub> {glass} + 5 Ti → Ti<sub>5</sub>Si<sub>3</sub> + 3 O<sub>2</sub>). The interfaces with optimum adhesion exhibit a nanostructured interfacial silicide layer. In indentations performed on polished cross sections of these coatings, cracks did not propagate along the glass/metal interface, but rather tended to be driven into the glass coating (Fig. 1), which is a qualitative indication of a strong glass/metal adhesion. If a thin TiO<sub>x</sub> or TiN<sub>x</sub> layer remains at the interface, the coatings

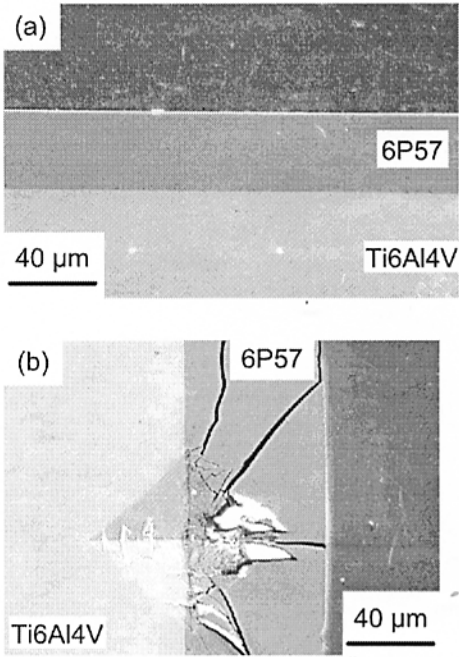


Fig. 1. a) Cross section of a 6P57 coating fired in air (800 °C/30 s). b) Vickers indentation (0.2 kg load in ambient air) at the 6P57/Ti6Al4V interface. The cracks did not propagate along the glass/metal interface, but are driven into the coating, suggesting a strong glass/metal adhesion.

easily delaminate. Excessive reaction is also undesirable because it results in the generation of bubbles in the coating resulting from the excess of liberated oxygen and the formation of a thick and brittle silicide layer at the interface.

A TEM image of the glass 6P57/Ti6Al4V interface annealed at 800 °C for 30 s is shown in Figure 2. An interfacial Ti<sub>5</sub>Si<sub>3</sub> layer, ~150 nm thick, can be observed. The layer

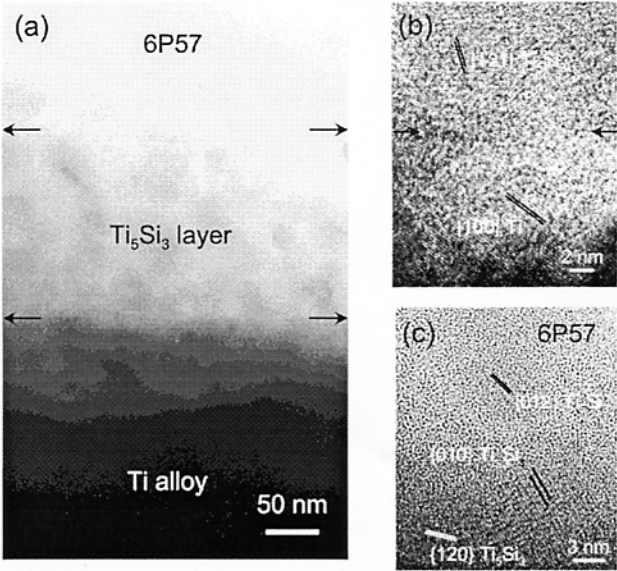


Fig. 2. HRTEM analysis of a 6P57 coating fired in air (800 °C/30 s) showing the presence of a Ti<sub>5</sub>Si<sub>3</sub> interfacial layer. a) General view. b) Ti6Al4V/Ti<sub>5</sub>Si<sub>3</sub> interface. c) 6P57/Ti<sub>5</sub>Si<sub>3</sub> interface.

is divided into two regions: a continuous nanocrystalline layer in contact with the alloy and, on top of it, a zone with isolated Ti<sub>5</sub>Si<sub>3</sub> nanoparticles dispersed in the glass. The appearance of isolated particles on the TEM image can also result from the growth of elongated silicide grains, or dendrites, from the continuous layer into the glass. These dendrites may appear as isolated particles wherever they intersect the cross section. Figure 2b corresponds to the Ti<sub>5</sub>Si<sub>3</sub>/alloy interface, where the lattice fringes of Ti {100} and Ti<sub>5</sub>Si<sub>3</sub> {121} are visible. A good lattice match exists between them, which can help in obtaining good adhesion. The glass/Ti<sub>5</sub>Si<sub>3</sub> interface is shown in Figure 2c. The size of the particles is in the range of ~20 nm, and Ti<sub>5</sub>Si<sub>3</sub> lattice fringes can be observed ([120], [010], and [012]).

All our attempts to coat Ti6Al4V with a single layer of Bioglass failed, because of cracking and excessive crystallization. The experiments have shown that there is a narrow range of glass compositions in the SiO<sub>2</sub>-CaO-MgO-Na<sub>2</sub>O-K<sub>2</sub>O-P<sub>2</sub>O<sub>5</sub> system that can be used to coat Ti or Ti6Al4V and that also form apatite (the mineral component of the bone) during in-vitro tests in simulated body fluid (SBF) (as displayed in Fig. 3).<sup>[13]</sup> Glasses with silica contents above this range are able to form adherent coatings, but are not bioactive. Glasses with less SiO<sub>2</sub> have enhanced dissolution rates and precipitate apatite readily when immersed in SBF. During in-vivo studies, bone grows into po-

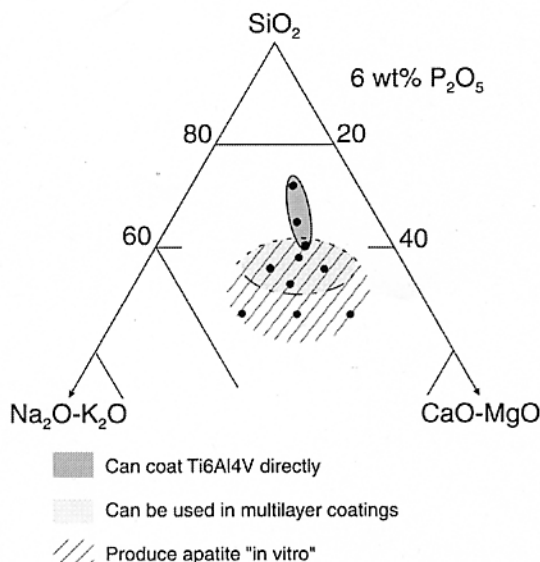


Fig. 3. Compositional triangle showing the range of glass compositions that can coat directly Ti6Al4V vs. those that can be used in graded coating without cracking. The range of bioactive compositions is also indicated.

rous glass 6P55 as the material is progressively substituted by mature osseous tissue.<sup>[14]</sup> However, their CTE is too high compared to that of Ti and Ti6Al4V, and large thermal stresses are induced during processing, resulting in cracked coatings. Thus, one motivation for developing graded coating is to reduce thermal stresses, so that a coating can be developed that has both a bioactive surface and an excellent adhesion to the metal. As an added advantage, the composition of the glass joining the metal can be such that its dissolution rate in body fluids is very limited (by using glasses with high  $\text{SiO}_2$  content), thus enhancing the long-term coating stability.

The basic enameling technique developed in this work was modified to prepare graded coatings. Layers of glasses with different compositions and mixtures of glass and HA were sequentially deposited on the metal and then fast-fired under the conditions that provide optimum adhesion for the glass in contact with the alloy. The elemental EDS analysis along the cross sections of multilayer coatings reveals a stepwise variation in the concentration of the glass components (with the exception of  $\text{Na}_2\text{O}$ ) that corresponds to the composition of the different deposited glass layers (Fig. 4). The concentration of  $\text{Na}_2\text{O}$  varied gradually across the coating.

The control of the gradient development during firing is critical in the fabrication of layered coatings. Two mechanisms control the development of the gradient during heat treatment: interdiffusion of the glass components and infiltration of one glass layer into another. Infiltration between adjacent glass layers can occur as a result of the different softening points ( $T_s$ ) of the glasses. Glasses with lower  $\text{SiO}_2$  soften at lower temperature and, consequently, may infiltrate during heating a neighboring layer with higher silica content, which remains porous. The EDS analysis indicates

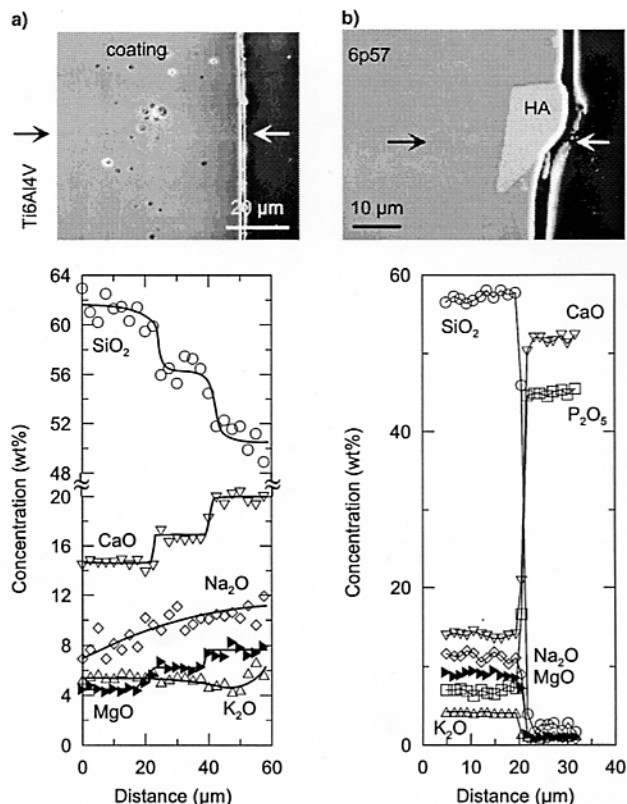


Fig. 4. a) EDS elemental analysis along the cross section of a graded coating (6P61/6P55/6P53) fired in  $\text{N}_2$  for 800 °C, 1 min. b) EDS line analysis of the 6P57/HA interface in a coating fired in air at 820 °C for 30 s.

that because of the short firing times, infiltration and interdiffusion (with the exception of sodium) are limited to a few micrometers ( $<5 \mu\text{m}$ ). The diffusion coefficient of  $\text{Na}^+$  in soda-lime-silicate glasses ranges typically between  $10^{-6}$ – $10^{-7} \text{ cm}^2/\text{s}$  at temperatures between 800–900 °C and is several orders of magnitude higher than for the other components.<sup>[15]</sup> During firing, sodium interdiffusion is fast enough to generate a smooth  $\text{Na}_2\text{O}$  profile even for the short firing times used in this work (Fig. 3). The short firing times and low temperatures also allow the introduction of synthetic hydroxyapatite particles to improve bioactivity without any deleterious reaction (Fig. 3b).<sup>[16]</sup> Bi-layered coatings containing an internal layer ( $\sim 50 \mu\text{m}$  thick) of glasses 6P61 or 6P68, and an external layer ( $\sim 20 \mu\text{m}$  thick) formed by a mixture of glasses 6P61 or 6P57 and HA (with hydroxyapatite contents as high as 50 wt.-%) have been prepared without cracking or delamination. The use of several firing steps (one for each deposited layer) was also investigated, but the successive heat treatments resulted in overreaction at the glass/metal interface.

During in-vitro testing in SBF, calcium phosphate crystals precipitated on the coatings with surface silica contents lower than 57 wt.-%. Fourier transform infrared spectromicroscopy (FTIRSM) and X-ray analysis of the precipitates identify them as apatite (Fig. 5). The apatite grows in the form of oriented nanocrystals, with the  $c$ -axis perpendicular

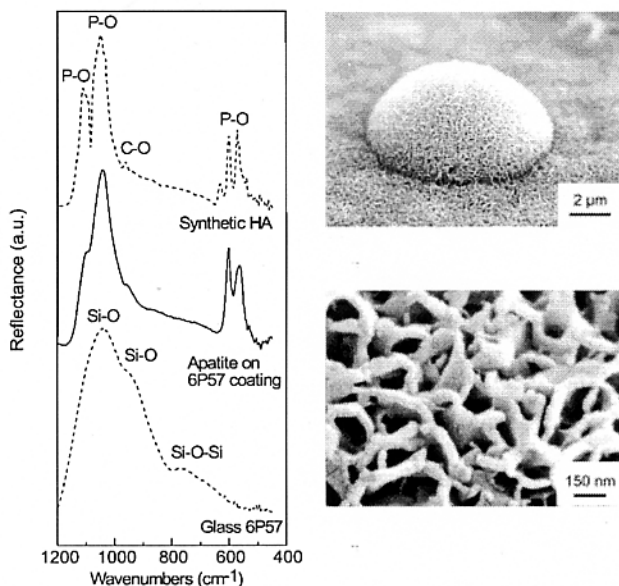


Fig. 5. Apatite crystals that formed on the surface of a 6P57 coating after immersion in SBF for 30 days and their FTIRSM analysis. FTIRSM analysis of the synthetic HA used in this work and of glass 6P57 is also shown (peak assignment from ref. [22]).

to the substrate. The EDS analysis indicates that the apatite crystals incorporate 1 to 5 wt.-% MgO in their structure substituting for CaO. The mechanism of apatite formation is similar to the one described by Hench for glasses in the  $\text{SiO}_2\text{-CaO-Na}_2\text{O-P}_2\text{O}_5$  system.<sup>[17]</sup> This involves the leaching of CaO,  $\text{Na}_2\text{O}$ , and  $\text{P}_2\text{O}_5$ , and the formation of an amorphous calcium phosphate layer on which the apatite crystallizes. One advantage of the graded coatings is that by introducing HA-containing layers, the time required for apatite precipitation in vitro is reduced on average by half with respect to the times observed in single-layer glass coatings. The preliminary data indicates that the HA particles act as nucleation centers for the precipitation of new apatite. The closed structure of glasses with high silica content impedes the ion exchange necessary for apatite formation.<sup>[18]</sup> Our analysis indicates that no appreciable corrosion of 6P61 or 6P68 glass layers in SBF occurs for times up to 4 months, suggesting that their use in multilayer coatings can provide effective protection of the alloy from the body fluid, increasing the long-term stability of the coating.

The low glass/metal thickness ratio of the coatings ( $<1:20$ ) suggests that only a moderate relief of thermal stress on the external layer of multilayered coatings should be expected using the graded approach. Nevertheless, for thin coatings, a gradient can markedly diminish the driving force for either cracking or delamination. In addition, stresses are singular where interfaces intersect the edges of samples, explaining why cracking originates at such places. These singularities are eliminated by continuous gradients; with multilayer coatings, the strength of these singularities is diminished inversely with the number of layers.<sup>[19]</sup> The mechanical benefits of the graded approach allowed the preparation of layers with lower silica content (which con-

sequently made the layers more bioactive) or with glass/HA composites, maintaining strong adhesion at the glass/metal interface. Layers with silica content as low as 53 wt.-% or containing as much as 50 wt.-% of synthetic hydroxyapatite were successfully prepared using the multilayer method. Because of the thermal expansion mismatch and the resulting high thermal stresses generated during processing, all those layers cracked or delaminated when applied directly to the alloy.

It is possible to design gradients for which the residual stress distribution of the coating change from a surface under tension to a compressive stress for the glass in contact with the metal (using glasses in contact with the substrate with lower thermal expansion than the alloy). Recent theoretical and experimental studies have shown that such stress distributions are effective in arresting crack growth. In this way, coatings are more resistant to fatigue and can be fabricated with more reliable mechanical properties.<sup>[20,21]</sup> Owing to their low silica content, single-layer bioactive coatings are under tension, and they are prone to corrosion. During in-vitro tests, cracks grew in the coating, reaching the metal and initiating delamination (Fig. 6). By using the graded approach, glass layers with high silica content that are under compression and more resistant to corrosion (e.g., glass 6P68) can be placed in contact with the metal. During immersion in SBF for times up to 4 months, the high-silica layers effectively arrested the growth of cracks that formed at the coating surface due to stress corrosion before they reached the glass/metal interface.

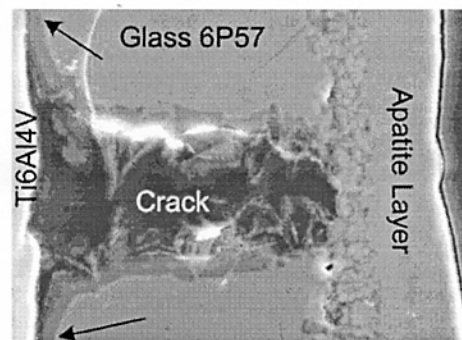


Fig. 6. Crack formed in a single-layer 6P57 coating after 2 months immersion in SBF. The crack reached the metal and corrosion has been initiated at the glass/metal interface.

In conclusion, because all attempts to coat the alloy with Bioglass failed, a new family of silicate-based glasses with composition tailored to match the thermal expansion coefficient of Ti and Ti6Al4V has been developed to coat metallic implants, using a simple enameling technique. Only a narrow range of compositions in the  $\text{SiO}_2\text{-CaO-MgO-Na}_2\text{O-K}_2\text{O-P}_2\text{O}_5$  system are able to form apatite during in-vitro tests and that can be used to coat Ti and Ti6Al4V. Because of their high silica content, the bioactivity of these compositions is limited. To better adjust the properties of the coating (in particular, to enhance bioactivity and increase chemical and mechanical stability), a multilayer ap-



proach has been used to fabricate graded glass coatings on Ti6Al4V. Graded coatings with a corrosion-resistant glass composition protecting the metal and surface silica contents as low as 53 wt.-% were successfully fabricated. Also, layers containing as much as 50 wt.-% of synthetic hydroxyapatite were prepared with no appreciable degradation of the HA. The preliminary adhesion tests indicate a strong glass/metal bond, while at the same time the coatings form apatite on their surfaces when tested in vitro. The multilayer coating approach used in this work provides an exciting prospect for engineering new implant coatings.

## Experimental

The glasses were fabricated following a conventional procedure described elsewhere [14], and their thermal properties were evaluated by dilatometry. The coatings were prepared using a standard enameling technique in which glass or glass/HA suspensions in ethanol (particle size <20  $\mu\text{m}$ ) were sequentially deposited on Ti6Al4V plates (99% purity,  $15 \times 10 \times 1 \text{ mm}^3$ ) to prepare the required multilayers. After the deposition, the samples were dried 20 h in air at 60°C to eliminate organics and fired in air or  $\text{N}_2$  to make the glass flow and adhere to the metal. The heating rates varied between 25 and 40°C/min, and firing temperatures ranged between 800 and 840°C, with higher temperatures for the glasses with higher softening points. The optimum firing times varied between 0 and 60 s in air and 1 and 15 min in  $\text{N}_2$ . The final coating thickness ranged between 50 and 70  $\mu\text{m}$ .

Samples for HRTEM were prepared by cutting cross sections of the glass/Ti6Al4V interface. The sections were ground to a thickness of ~100  $\mu\text{m}$  with emery paper, and then fixed onto a Cu mesh with 3 mm diameter. The disks were polished with a dimple grinder (Gatan, Model 656) to less than 20  $\mu\text{m}$  in thickness and milled by argon ion-milling (E. A. Fischione Instruments, Inc. Model 3000) at an accelerating voltage of 2 to 4 kV. HRTEM observations were performed with a 1250 kV electron microscope (ARM-1250 kV) having a point-to-point resolution of 0.12 nm.

The behavior of the glasses and coatings in SBF was studied by in-vitro tests. Glass plates and coatings (area  $\sim 10 \times 10 \text{ mm}^2$ ) were soaked in SBF [11] at a constant temperature of 36.5°C for different times up to 4 months. After soaking, the samples were analyzed by XRD, SEM with associated EDS and FTIRSM in the advanced light source (ALS) at the Lawrence Berkeley National Laboratory. The FTIRSM uses the synchrotron beam at the ALS as an external light source in a Nicolet Magna 760 bench with Nic-Plan IR Microscope, which allows focusing the beam in very small diameters with little loss of signal. With a 32 $\times$  objective, the full width, half maximum spot size is ~10  $\mu\text{m}$ ; this spot size becomes diffraction limited at longer wavelengths. The spectra were taken in the reflectance mode using a KBr beam splitter and an mercury cadmium telluride detector.

Received: January 25, 2000  
Final version: March 31, 2000

- [1] P. Ducheyne, *MRS Bull.* **1998**, 11, 43.
- [2] H. C. Slavkin, *J. Am. Dent. Assoc.* **1996**, 127, 1254.
- [3] C. L. Tisdell, V. M. Goldberg, J. A. Parr, J. S. Bensusan, L. S. Staikoff, S. Stevenson, *J. Bone Jt. Surg. Am. Vol.* **1994**, 76, 159.
- [4] J. C. Chae, J. P. Collier, M. B. Mayor, V. A. Surprenant, L. A. Dauphinais, *J. Biomed. Mater. Res.* **1992**, 26, 93.
- [5] S. R. Radin, P. Ducheyne, *J. Mater. Sci. Mater. Med.* **1992**, 3, 33.
- [6] K. A. Gross, V. Gross, C. C. Berndt, *J. Am. Ceram. Soc.* **1998**, 81, 106.
- [7] W. R. Laceyfield, in *An Introduction to Bioceramics* (Ed: L. L. Hench, J. Wilson), World Scientific, Singapore **1993**, pp. 223–238.
- [8] B. Kasemo, J. Gold, *Adv. Dent. Res.* **1999**, 13, 8.
- [9] J. S. Moya, *Adv. Mater.* **1995**, 7, 185.
- [10] A. Mortensen, S. Suresh, *Int. Mater. Rev.* **1995**, 40, 239.
- [11] S. Suresh, A. Mortensen, *Int. Mater. Rev.* **1997**, 42, 85.
- [12] L. L. Hench, E. C. Ethridge, *J. Am. Ceram. Soc.* **1991**, 74, 1487.
- [13] J. Gamble, *Chemical Anatomy, Physiology and Pathology of Extracellular Fluid*, Harvard University Press, Cambridge, MA **1967**.
- [14] L. Devesa, A. Pazo, C. Santos, A. Martinez, F. Guitian, J. S. Moya, *Acta Mater.* **1998**, 46, 2559.

- [15] W. D. Kingery, H. K. Bowen, D. R. Uhlman, *Introduction to Ceramics*, 2nd ed., Wiley, New York **1976**, pp. 257–263.
- [16] A. Pazo, C. Santos, F. Guitian, A. P. Tomsia, J. S. Moya, *Scr. Mater.* **1996**, 34, 1729.
- [17] L. L. Hench, Ö. Andersson, in *An Introduction to Bioceramics* (Ed: L. L. Hench, J. Wilson), World Scientific, Singapore **1993**, pp. 41–62.
- [18] M. W. G. Lockyer, D. Holland, R. J. Dupree, *J. Non-Cryst. Solids* **1995**, 188, 207.
- [19] F. Erdogan, *Compos. Eng.* **1995**, 5, 753.
- [20] D. J. Green, R. Tandon, V. M. Sglavo, *Science* **1999**, 283, 1295.
- [21] J. F. Bartolome, J. S. Moya, J. Requena, J. L. Lorca, M. Anglada, *J. Am. Ceram. Soc.* **1998**, 81, 1502.
- [22] C. Y. Kim, A. E. Clark, L. L. Hench, *J. Non-Cryst. Solids* **1989**, 113, 195.

## A CO<sub>2</sub> Sensor Based on a Trivalent Ion Conducting Sc<sub>1/3</sub>Zr<sub>2</sub>(PO<sub>4</sub>)<sub>3</sub> Solid Electrolyte\*\*

By Shinji Tamura, Nobuhito Imanaka,  
Masayuki Kamikawa, and Gin-ya Adachi\*

In recent years, global warming caused by CO<sub>2</sub> gas emission has become a very serious problem, and the effective suppression of CO<sub>2</sub> generated in various industries is urgently required. In order to effectively reduce the amount of CO<sub>2</sub> gas emitted into the atmosphere, on-site monitoring and control of CO<sub>2</sub> generated from each emitting site are required. To accomplish this target, commonly used methods such as infrared spectroscopy are not suitable because of the large size of the set-up. Therefore, compact sensors that can be installed at every site are required. Until now, semiconducting<sup>[1–3]</sup> and solid electrolyte<sup>[4–9]</sup> materials have been proposed for use in compact CO<sub>2</sub> sensors. However, with the sensors using semiconductors, the influence of gas species other than CO<sub>2</sub> can not be avoided, since their detecting mechanism is based on gas adsorption on the semiconductor's surface. In contrast, solid electrolyte sensors, in general, have the unique characteristic that only one ion species can migrate in the solid. Solid electrolytes are used for various practical applications such as oxygen gas sensors, based on yttria-stabilized zirconia (YSZ), and heart pacemakers, etc. Recently, a CO<sub>2</sub> sensor composed of a Li<sup>+</sup>-conducting solid electrolyte and YSZ with Li<sub>2</sub>CO<sub>3</sub> as an auxiliary electrode was reported.<sup>[8,9]</sup> The CO<sub>2</sub> concentration was measured by the electromotive force (EMF) output, which depends strongly on the activity of the Li<sub>2</sub>O formed at the interface between the Li<sup>+</sup> ion conductor and

[\*] Prof. G. Adachi, S. Tamura, Dr. N. Imanaka, M. Kamikawa  
Department of Applied Chemistry, Faculty of Engineering  
Osaka University  
2-1 Yamadaoka, Suita, Osaka 565-0871 (Japan)  
E-mail: adachi@chem.eng.osaka-u.ac.jp

[\*\*] The present work was partially supported by a Grant-in-Aid for Scientific Research No. 09215223 on Priority Areas (No. 260), Nos. 06241106, 06241107, and 093065 from The Ministry of Education, Science, Sports and Culture. This work was also supported by the "Research for the Future, Preparation and Application of Newly Designed Solid Electrolytes (JSPS-RFTF96P00102)" Program from the Japan Society for the Promotion of Science.